Journal of Geography and Geology; Vol. 11, No. 3; 2019
ISSN 1916-9779 E-ISSN 1916-9787
Published by Canadian Center of Science and Education

Effect of Extreme Weather Events on the Sedimentation of the Bay of Samaná, Dominican Republic (1900–2016)

Delanoy Ramón A.[1], Díaz-Asencio Misael[2] & Méndez-Tejeda, Rafael[3]

[1] Instituto de Física, Facultad de Ciencias, Universidad Autónoma de Santo Domingo, Ministerio de Educación Superior Ciencia y Tecnología. República Dominicana. Av. Alma Master. Apartado Postal 1355. Santo Domingo. RD.

[2] Division of Oceanology. Ensenada Center for Scientific Research and Higher Education. México. Tijuana No. 3918, Zona Playitas, CP. 22860, Ensenada, B.C. México

[3] Research Laboratory in atmospheric science. University of Puerto Rico at Carolina. Puerto Rico. Po. Box 4800. Carolina Puerto Rico. 00984

Correspondence: Méndez-Tejeda, Rafael, Research Laboratory in atmospheric science. University of Puerto Rico at Carolina. Puerto Rico. Po. Box 4800. Carolina Puerto Rico. 00984. E-mail: rafael.mendez@upr.edu

Received: September 5, 2019 Accepted: September 26, 2019 Online Published: September 30, 2019

doi:10.5539/jgg.v11n3p56 URL: http://dx.doi.org/10.5539/jgg.v11n3p56

Abstract

The Bay of Samaná, formed by tectonism and sedimentation, is delimited to the north by the peninsula of the same name, to the south by the north slope of the Eastern Mountain Range and Los Haitises National Park, to the east by the Atlantic Ocean, and to the west by the ancient Gran Estero, today the Lower Yuna. There follows a process of continuous degradation by the existing tectonic forces and the sediment contributions by the Yuna, Yabón, and La Yeguada rivers to the south as well as by the landslides of the mountainous area of the Samaná Peninsula, during periods of storms and hurricanes. The coastal area of Samaná Bay has altered by 2.17 km^2 at the mouth of the Yuna River from 2003–2015. The high turbidity level has affected coral reefs and marine species. The mangroves are lost faster than they are regenerated by the coastline's change. Variations in the elemental compositions of calcium and iron show the terrigenous influence on the dynamics of the bay during Extreme Weather Events (EWP) in the river basins that flow into it. Abrupt changes in the rainfall regime produced an equal change in the estuary sedimentation regime, according to the 210Pb. In the 2007–2016 period, a column of sediment that reached 38 cm and a 12 cm to 8.4 km column were deposited 4 km southeast of the municipality of Sánchez and east of the mouth of the Yuna River. The Sedimentary Accumulation Rate is very high, and the content of heavy metals exceeds the threshold values of Table SQuirt.

Keywords: Sedimentation, Bay of Semaná, Extreme Event, Dominican Repúblic

1. Introduction

The island Hispaniola, located in the arch of the Greater Antilles in the Caribbean region, has its origin in the region's tectonic movements and volcanism. Inside it has several active geological faults (Mann et al., 1984), the most important being the northern one on the northern edge of the Caribbean plate where it collides with the North American plate (Bionini et al., 1984). In the northeastern section, in the study area, the Bay of Samaná, is influenced by a zone of subduction (Figure 1), where tectonic movements are frequent, often producing small earthquakes. In the Bay of Samaná on August 4, 1946, an earthquake of magnitude 8.1 on the Richter scale, the largest earthquake in the Dominican Republic, was recorded by instrumental seismology (Delanoy, 1996). The region moves according to the shifting of the Caribbean plate about 37 mm per year, which represents a displacement of 63 cm in 20 years (Bionini et al., 1984) in the region, the Cibao fault, and the North. The Yabón fault, the most important of the eastern mountain range, meets the Cibao fault and the Septentrional fault in Samaná Bay, giving rise to a very complex area from the point of view of structural geology and tectonics (Bird, 1980). Coastal displacements by the tectonic forces that affect the region generate the formation of lagoons, which results in the Atlantic Ocean gaining ground while the bay loses ground (Brink et al., 2004).

Figure 1. Map of the Caribbean region. The box is the location of the Bay of Samaná in the Dominican Republic

Source: https://en.wikipedia.org/wiki/Battle_of_the_Caribbean, https://www.viajarcaribe.es/blog/mapas/

The sediments caused by landslides on the peninsula's escarpments and the drags of the rivers and streams in the northern part of the bay (Eptisa, 2004) during storms and hurricanes are important entities for its degradation (Dolan, 1991). The greatest contributions come from the waters of the Yuna, Yabón, Caño Hondo, and Yeguada rivers that flow south into the bay. The coastal area to the south has been changing due to the contributions of large masses of soils that have been washed away. The use of nuclear and conventional analytical techniques has allowed the reconstruction (Alonso-Hernández et al., 2016) of the degradation process and the factors linked to the sediments in the period from 1900–2016.

The sedimentation rate, physicochemical composition, enrichment, and age are information that we can obtain through these techniques. These parameters are always linked to the displacement of soil masses either by landslides or erosion during heavy rains, which are usually linked to storms or hurricanes and are considered Extreme Weather Events (EWP). Since the 90s, there has been an increase in EWP (NCA, 2018), which affected the Bay of Samaná during the 2004–2012 period, an incidence predominant in the La Niña period (Null, 2017). EWP are frequent in the Dominican Republic because of their location in relation to the routes of tropical waves, hurricanes, and storms that form in the south-central zone of the tropical Atlantic and that are dragged by the trade winds to the northwest, as well as CRCC's (Mendez-Tejeda, 2017). The rivers' sediment contributions during the storms of 2004–2012 were very remarkable (Delanoy et al., (2017). The same happened with the passage of hurricanes Irma and Maria in September 2017.

The Bay of Samaná holds an important economic importance for the Dominican Republic. It is a place to sight humpback whales which, in late winter and early spring, remain in the bay's warm waters to breed. Tourism, fishing, and agriculture are the most important economic sources of livelihood in the towns of Sánchez, Samaná, Sabana de la Mar, and Miches. These are some of the reasons for the importance of studying sedimentation as an element of the ecosystem's (coastal zone and biodiversity) degradation. The study of sediments can provide current and past information since they record the geological and hydrological phenomena of the basin from where they are transported by river waters or wind. The use of nuclear techniques as tools allows reconstructing the past of a basin's activities. Through dating with 210Pbex, a natural radiotracer of the 238U disintegration chain, it is possible to reconstruct the past (up to 150 years), using sediments as environmental files (Alonso-Hernández, et al., 2016, IAEA 1989, Salamanca et al., 2003, Rodriguez, et al., 2013). This period covers industrial development activities and the population growth in the region in the last eight decades (National Bureau of Statistics, Dominican Republic).

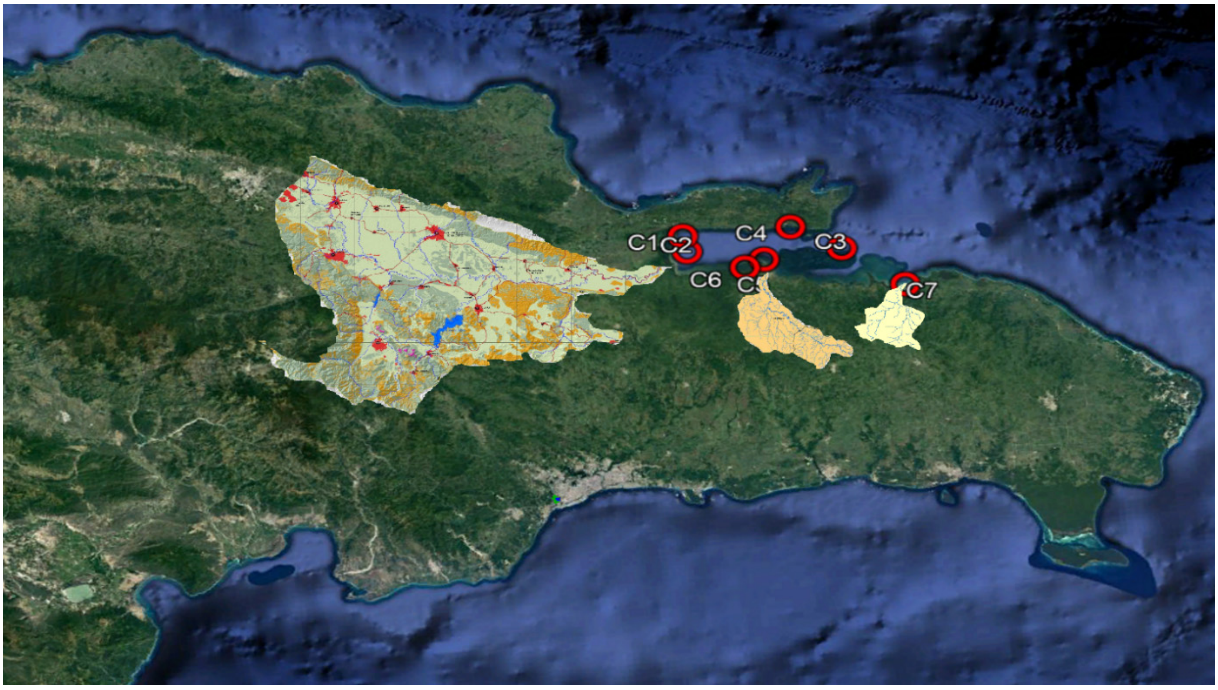

Figure 2. Map of the Dominican Republic. The light-colored areas correspond to the basins of the three main rivers that flow into the Bay of Samaná. Source: Google Earth, Ministry of Environment, Dominican Republic

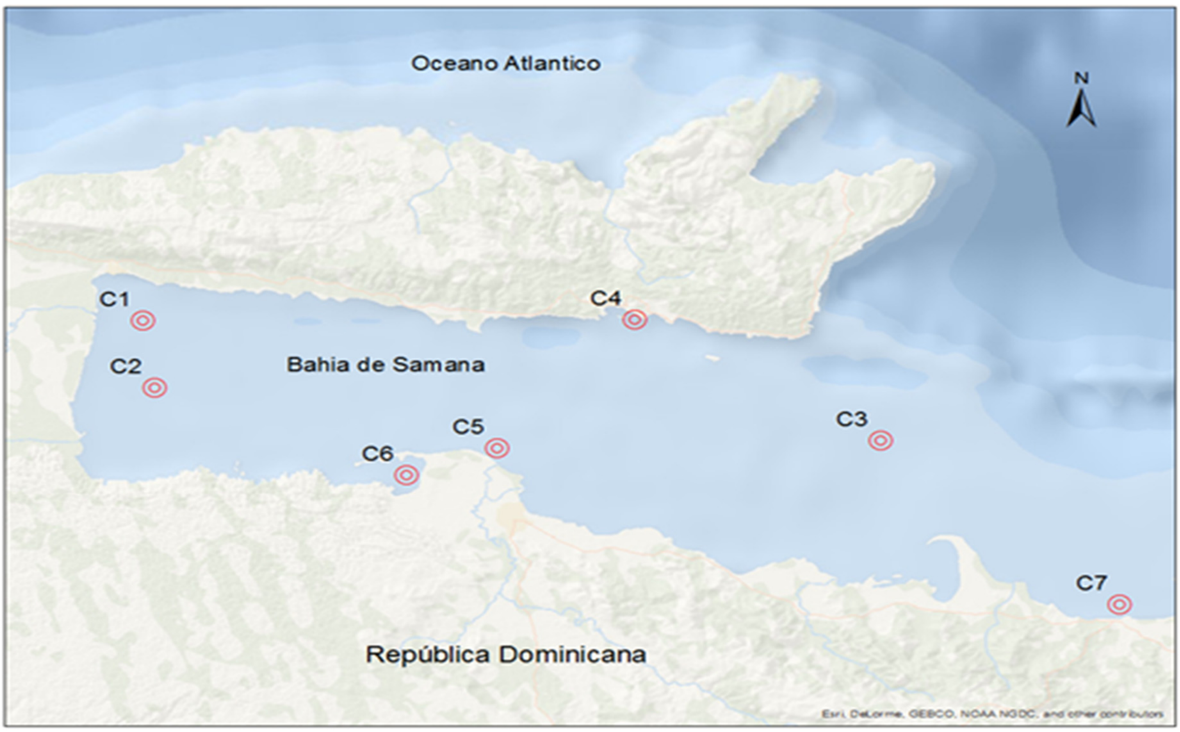

Figure 3. The places where the cores were taken in the area of influence of the rivers that flow into the Samaná Bay

Source: Google Earth

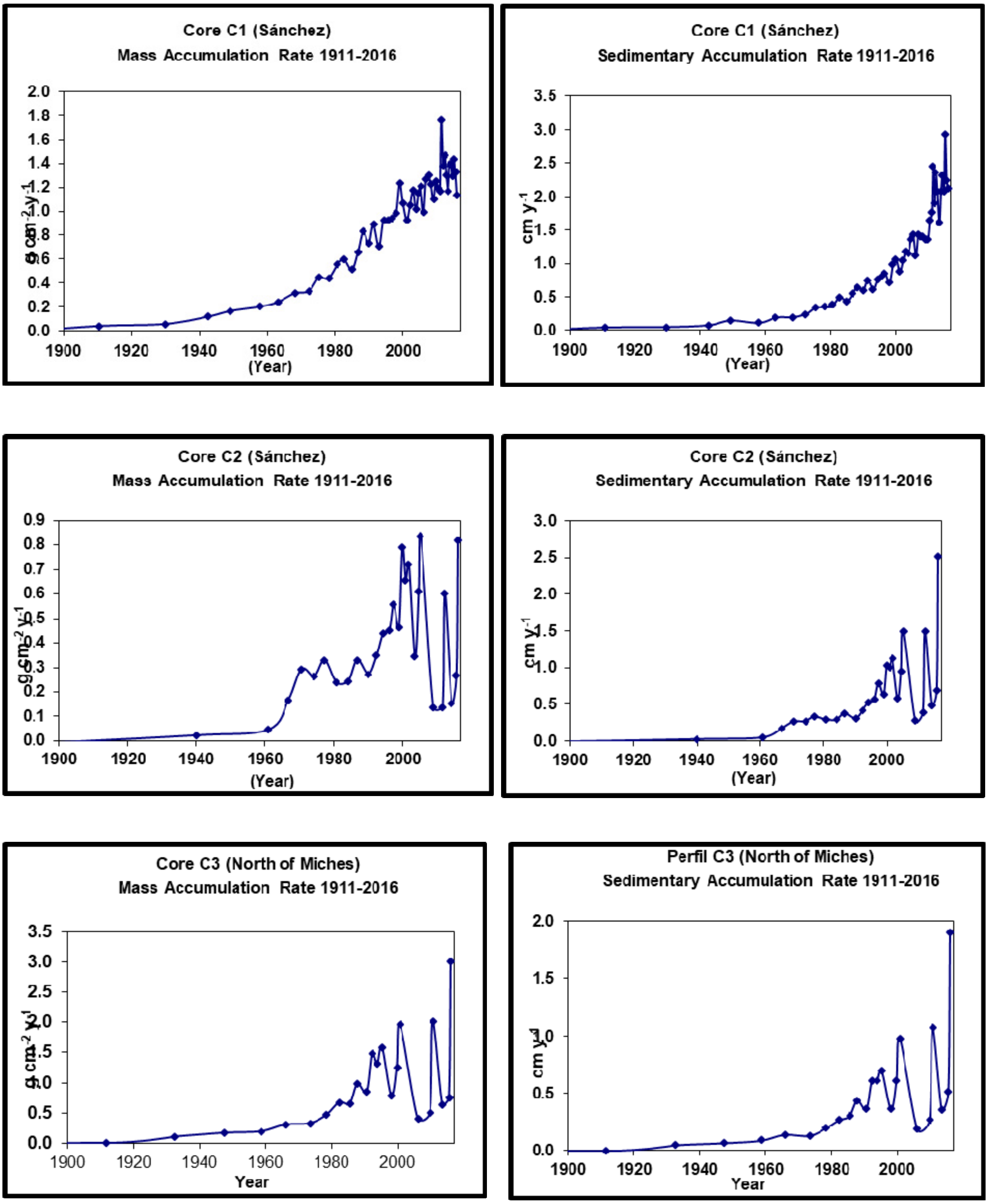

Figure 4. Sedimentary and Mass Accumulation Rate (MAR) according to the lead-210 dating of cores C1, C2, and C3

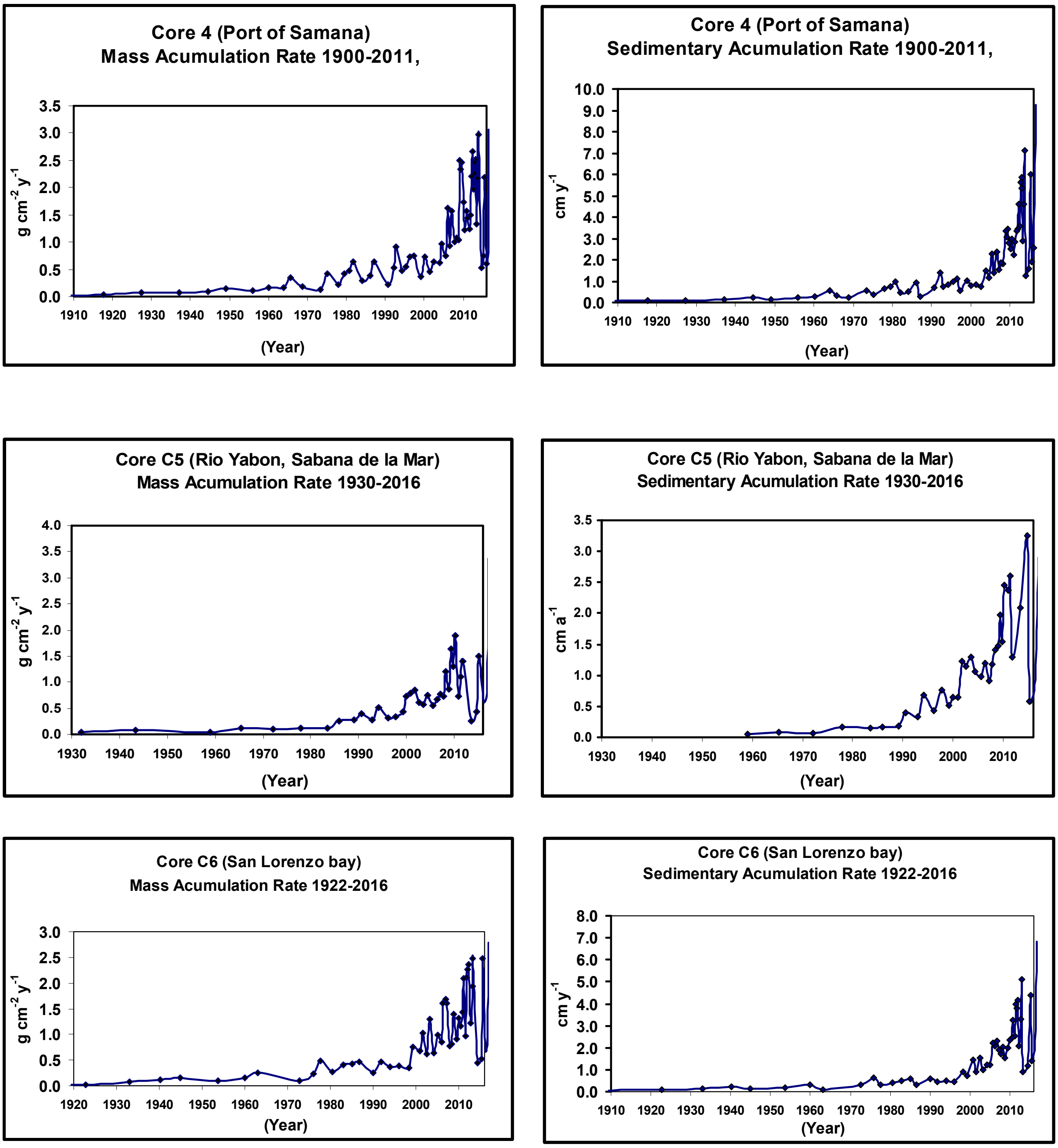

Figure 5. Sedimentary and MAR according to the lead-210 dating of cores C4, C5, and C6

2. Methods

2.1 Study Region

Core samples were taken at the different mouths of the rivers, the Yuna River and its tributaries the Camú and Jaya rivers cross the central Cibao region, collecting the waters of the Monseñor Noüel, Duarte, Sánchez Ramírez, and La Vega provinces, depositing their waters and eroded soils in the Bay of Samaná. In these provinces are important human settlements dedicated to agriculture, livestock, and mining that contribute to soil erosion and water pollution. Many of the waters used by domestic and hotel services in Samaná and Sánchez, towns located north of the bay, are also discharged to the water sources without treatment and contain metals and solid waste. To the south of the bay are the towns of Sabana de la Mar and Miches, which are related to the sediments that come from the rivers Yabón and La Yeguada, respectively. The main tributaries coming from the north side are the Majagual River and a series of small streams between the towns of Majagual and Sánchez (from north to south with little distance between: El Rancho streams, Los Chicharrones, La Jagua, Agua Buena, Las Canoas, La Cabilma, Los Naranjos, and Los Remedios). Several of these tributaries pour their waters into the Yuna near the mouth. Other tributaries are located between the towns of Sánchez and Punta Balandra, from north to south, with little distance between the Punta Gorda, Higüero, Salado, Hondo, Juana Vicenta, Las Flechas, and Los Limones streams and the Santa Capuza, Los Cocos, and the Bushi and Balandra rivers.

2.2 Yuna-Camu River

The Yuna river basin covers the south-central, northeast, and part of the north-central Cibao region, a 5,253 km^2 area surrounded by a broad-leaved forest that occupies about 44% (2.311 km^2) of the basin. The remaining 56% is dedicated to four types of intensive agricultural crop uses (848.63 km^2), pastures (634.16 km^2), rice (607.27 km^2), and cocoa (530.74 km^2). The high zones of the Central Mountain Range and the Sierra de Yamasá are covered by 190.28 km^2 of coniferous forest (3.62%) (García-Senz et al., 2007, Hernaiz-Huerta et al., 2004).

2.3 La Yeguada River (Miches)

Located in the El Seibo province in the Yuma region, La Yeguada River flows into the municipality of Miches. The area of the basin is 53.7 km^2. Cocoa plantations are the main land use coverage in the La Yeguada river basin, comprising an area of 26.5 km^2 (49.3%). The humid and semihumid broad-leaved forests cover 19.33 km^2 (36%) of the basin. Grass is another land use, with about 7 km^2 (12.98%) of the basin (García-Senz et al., 2007).

2.4 Yabón River (Sabana de la Mar)

The Yabón River is located in the Higüamo and Yuma regions and the Hato Mayor and El Seibo provinces. The area of the basin is 370.61 km^2. The largest land use is for the cultivation of cocoa, about 107.24 km^2 (28.94%). Followed by the humid broad-leaved forest with 85.18 km^2 (22.99%) of the territory, grass occupies the third place with 71.83 km^2 (19.38%); the land uses with smaller extensions are: dry scrub, coconut, intensive cultures, among others (García-Senz et al., (2007).

3. Results

The results of the seven cores are shown in the following tables and graphs using techniques with X-ray fluorescence spectrometry. Tables 1–9 contain some values of the majority and minority elements determined in the nuclei by X-ray fluorescence as well as the sedimentation rate determined by lead-210 dating (Lozano et al., 2011), relating it to the deposition date of the sediments in the mouths of the rivers Yuna, Yabón, La Yeguada, Samaná, and Caño Hondo and one taken inside the Bay of Samaná. This information is related to the sedimentation of the Bay of Samaná due to the dragging of soils during tornadoes, storms, and hurricanes. The increase in iron and calcium in the C1 core is related to the substitution of organic matter as it degrades (Table 3). The decreases in iron and calcium in sections 20, 52, and 70 were due to an increase in mercury concentration.

Potassium values are related to organic matter content and those associated with EWP (Tormenta Olga, 2007, Hurricane George, 1998 and Gert, 1981), according to the date and the mass and sediment accumulation rate (Table 3, Figure 6). In the case of the Gran Estero and Lower Yuna, these sediments have historically been deposited by the river (Dolan, et al., 1998). Iron decreases with depth in the C2 core (Table 4), and calcium increases slightly. The C1 core showed an increase in calcium and the rate of sedimentation (1998) as a result of Hurricane George (Figure 5). This was taken in the area of influence of the Yuna River, as well as in the C1 core. The C3 core taken north of Miches, near a galleon loaded with mercury that sunk in the year 1724 during a storm (Fernández-Domingo, 2010), presented higher values of calcium than other nuclei and high mercury values (Table 5, Figure 7).

Table 1. Location, length, and depth of cores taken in the coastal areas of Samaná Bay, 2016–2017, for the study of sedimentation, dated with 210 lead and heavy metals in the last 100 years

Station	Latitude (N)	Longitude (W)	Depth (cm)	Prof. (m)	Site
C1	19.1926	69.5977	100	28	Desembocadura río Yuna-Barracote
C2	19.1460	69.5913	82	25	Desembocadura río Yuna
C3	19.1095	69.1805	46	12	Norte de Miches
C4	19.1933	69.3198	58	5	Puerto Samaná
C5	19.1041	69.3977	92	15	Río Yabón
C6	19.0851	69.4492	52	6	Río Caño Hondo
C7	18.9958	69.0452	20	6	Desembocadura Río Yeguada

Table 2. Comparison of the certified values of two reference materials BCR 277 and SRM 1944 and the values of these materials obtained with X-ray fluorescence spectrometry, to validate our results in the determination of the major elements and traces

Element	Unit	Certified value BCR277			Measured value XRF		
		Concentratión					
As	µg/g	18.3	±	1.8			
Cr	µg/g	188	±	14	188.0	±	9.0
Cu	µg/g	63	±	7.0	68.2	±	1.0
Ni	µg/g	130	±	8.0	131.0	±	4.0
Zn	µg/g	178	±	20	187.0	±	4.0
		Certified Value SRM 1944					
K	%	1.60	±	0.20	1.62	±	0.04
Ca	%	1.00	±	0.10	1.00	±	0.02
Fe	%	3.53	±	0.16	3.54	±	0.02
Cr	µg/g	266.0	±	24.0	267.40	±	16.18
Cu	µg/g	380.0	±	40.0	379.13	±	5.19
Zn	µg/g	656.0	±	75.0	656.17	±	3.35
As	µg/g	18.9	±	2.8	18.67	±	0.21
Br	µg/g	86.0	±	10.0	82.43	±	3.12
Hg	µg/g	3.4	±	0.5	3.30	±	0.14
Pb	µg/g	330.0	±	48.0	329.07	±	3.92

Table 3. Trace elements, Loss by ignition, % of Iron, % of Calcium, Sedimentation rate, Date, and EWP of the sections of core C1 corresponding to the mouth of the Yuna-Barracote river near the city of Sánchez during the period from 1888–2016. Only sections with mercury higher than 1.0 µg/g were considered

Proof (cm)	%PPI	%Ca	%Fe	Cr µg/g	Mn µg/g	Ni µg/g	Cu µg/g	Zn µg/g	Br µg/g	Hg µg/g	Pb µg/g	TAS cm/a	Sedimentation date	Storm Date
0	17.11	2.23	6.33	253.2	651.5	95.2	70.6	105.8	820.3	1.7	24.0	2.12	2016.1	
2	19.29	2.53	6.59	329.8	662.1	118.0	37.0	92.6	559.2	1.6	21.5	2.24	2015.6	
4	19.07	2.41	6.55	203.5	503.1	139.5	99.4	75.8	579.3	1.0	27.2	2.93	2015.2	Bertha 2014
18	17.11	2.12	6.53	169.9	527.9	111.5	71.6	100.7	437.3	2.8	23.7	1.90	2011.9	
20	16.85	2.22	6.09	242.5	543.9	108.1	113.9	89.3	474.6	3.9	25.6	2.45	2011.4	Irene 2011
22	17.41	2.51	6.59	341.9	623.2	133.1	121.3	340.6	439.3	1.9	43.1	1.76	2011.0	Tomas 2010
24	17.52	2.57	6.66	249.2	584.7	102.0	91.9	64.5	337.2	3.1	34.9	1.65	2010.4	Earl 2010
26	18.43	2.92	6.57	108.1	581.7	146.7	63.5	70.9	330.7	1.8	42.5	1.36	2009.8	
30	19.34	1.82	6.43	126.9	427.6	136.1	80.0	66.8	332.7	2.5	38.0	1.40	2008.3	Ike 2008
36	16.95	1.31	6.04	75.8	425.7	137.6	95.5	80.7	272.1	2.6	38.4	1.12	2006.2	
38	18.58	2.35	6.84	305.6	551.9	120.6	98.4	158.4	362.1	4.0	29.2	1.44	2005.3	Alpha 2005
40	16.61	1.61	6.26	121.5	509.6	130.4	134.9	70.4	391.2	2.8	39.9	1.37	2004.6	Jeanne 2004
42	17.24	2.09	6.86	230.4	753.7	118.0	52.2	110.5	311.2	5.4	45.5	1.15	2003.9	
46	19.13	2.08	6.62	251.9	652.2	158.9	63.5	109.2	183.9	3.3	22.0	1.04	2002.2	
52	13.64	2.21	6.95	192.8	713.6	131.2	87.1	214.2	265.6	2.9	33.8	0.98	1999.1	George 1998
62	17.19	2.03	6.79	251.9	741.5	137.6	99.4	46.8	233.1	3.0	34.6	0.62	1993.0	
64	17.10	2.60	7.08	211.6	720.5	144.5	52.2	83.2	202.8	2.7	30.3	0.75	1991.4	Hugo 1989
68	18.34	2.33	6.49	149.8	564.5	116.1	46.7	116.8	562.0	4.8	30.3	0.64	1988.4	
70	16.91	2.42	6.68	192.8	719.4	112.3	108.7	62.1	131.3	6.0	24.5	0.56	1986.8	
72	17.05	3.05	7.12	183.4	733.5	164.5	98.1	87.3	131.0	1.6	34.3	0.44	1985.0	
86	17.04	2.28	7.05	266.7	640.0	117.6	150.1	62.1	191.5	3.5	43.1	0.19	1963.1	
90	15.31	2.75	7.35	222.3	660.6	185.0	110.4	73.2	207.3	6.1	30.8	0.15	1949.2	Tsunami 1946
96	13.88	2.63	7.84	194.1	725.8	202.8	89.7	74.7	121.6	1.4	40.5	0.04	1910.5	

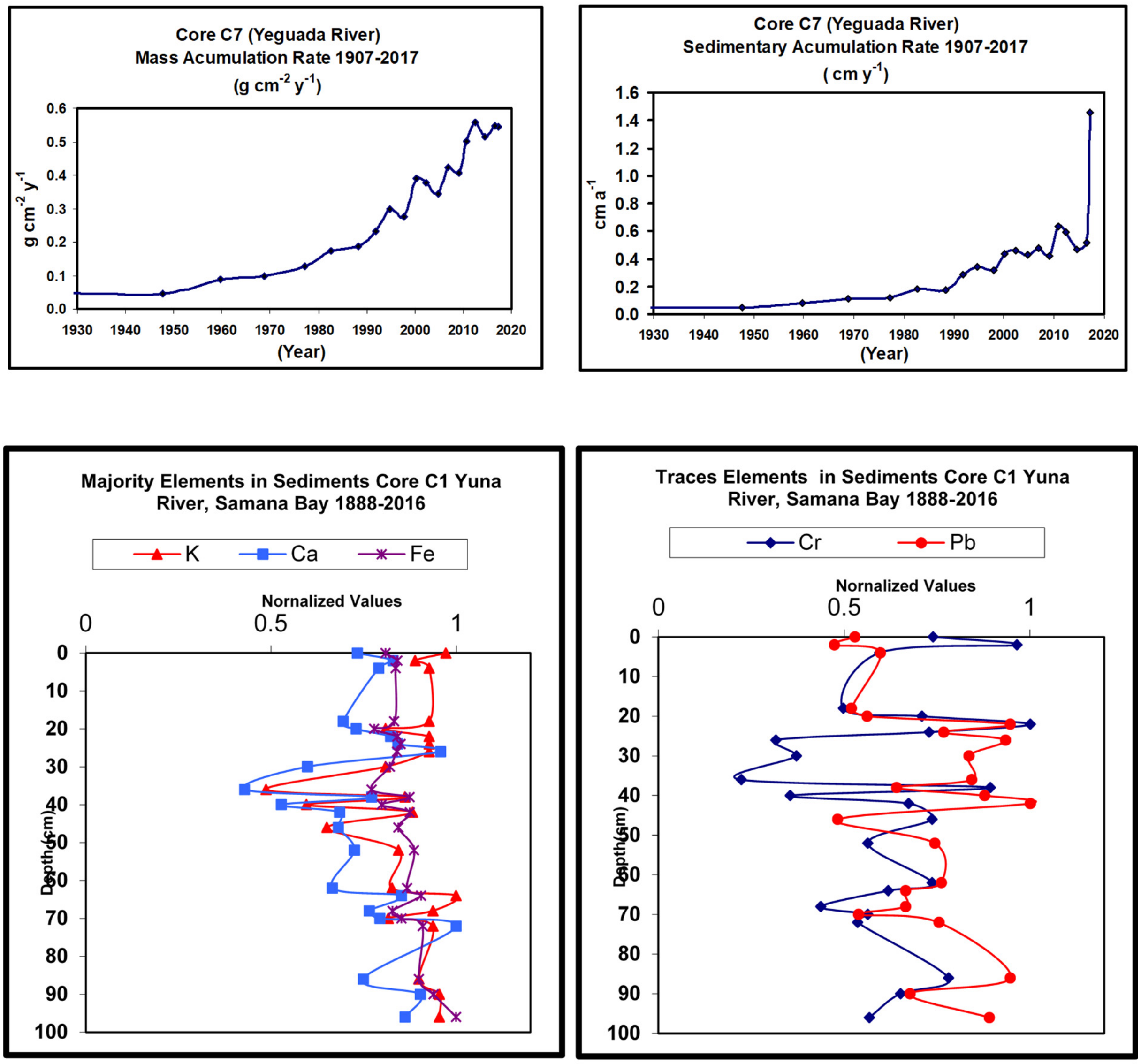

Figure 6. Sedimentary MAR (upper left), MAR (upper right) according to the lead-210 dating of the C7 core. Variation with the depth of the majority elements potassium, calcium, and iron (lower left) and minority elements chrome and lead (lower right) found in core C1 in the Sánchez province

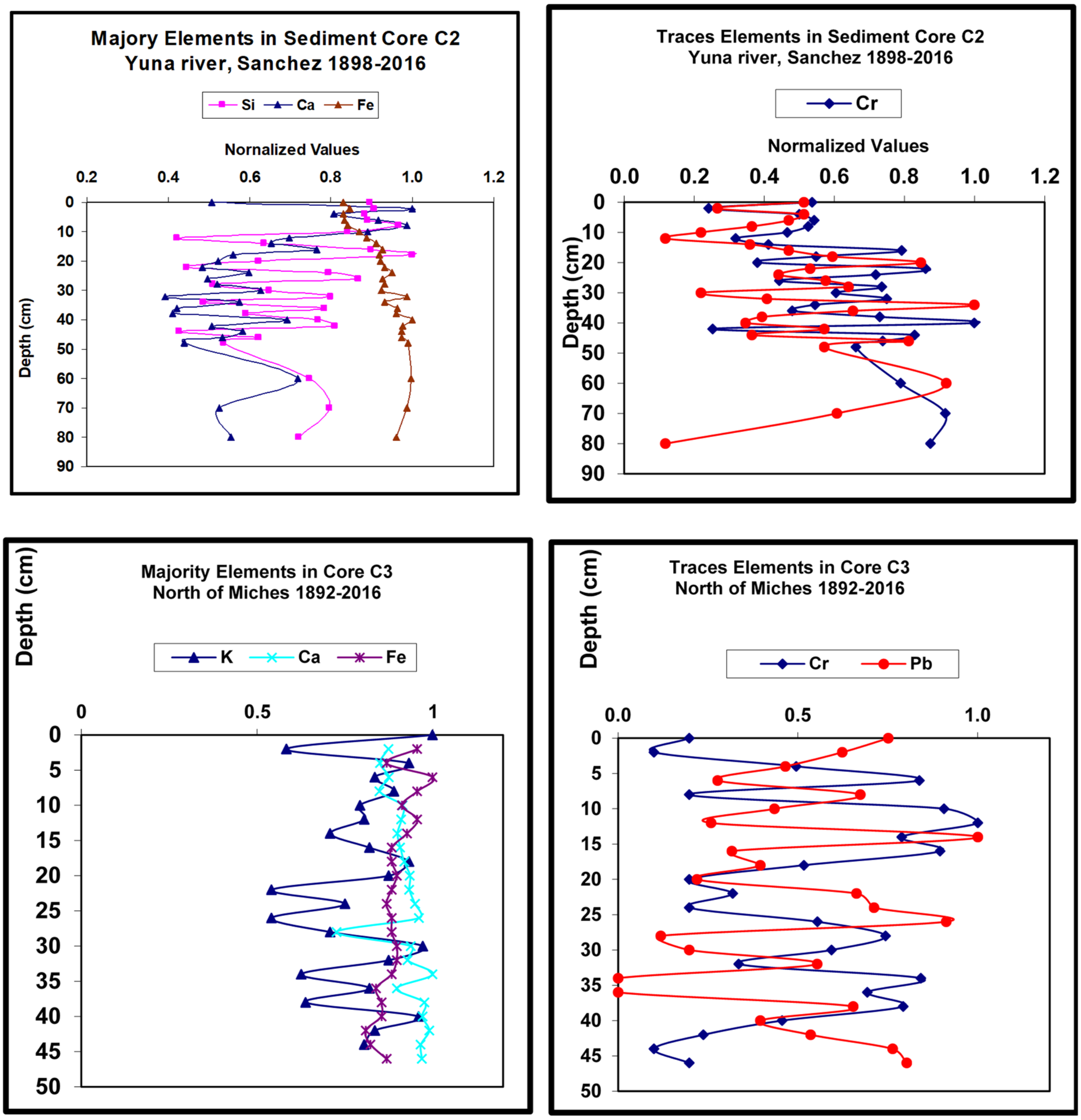

Figure 7. Relationship of the chemical elements with the depth in core C2 (majority: silicon, calcium, and iron; minorities: chromium and lead). Core C3 (majority: potassium, calcium, and iron; minority: chromium and lead)

Table 4. Trace elements, Loss by ignition, % of Iron, % of Calcium, Sedimentation rate, Date, and EWP of the sections of the core C2 corresponding to the mouth of the Yuna-Barracote river in the south of the Sánchez province during the period from 1898–2016

Proof (cm)	%PPI	%Ca	%Fe	Cr µg/g	Mn µg/g	Ni µg/g	Cu µg/g	Zn µg/g	Br µg/g	Pb µg/g	TAS cm/a	Sedimentation date	Storm Date
	14.82	1.76	5.1	190.1	412.3	86.1	44.3	119	1205.5	8.7	2.52	2016.1	
2	13.22	1.54	5.19	85.3	400.5	117.2	13.9	148.1	990.3	4.5	0.68	2015.7	Bertha 2014
4	12.56	1.69	5.11	176.6	423.4	118	47.8	216.3	877.4	8.7	0.48	2014.2	Gabrielle 2013
6	12.66	1.97	5.12	191.4	497.8	116.1	9.8	203.8	876	8	1.49	2012.1	Isaac 2012
8	13.73	2.02	5.17	186.0	466.5	114.9	34.4	182.3	837	6.2	0.38	2011.5	Irene 2011
10	13.65	2.18	5.34	164.5	543.1	85.4	49.8	119.4	840.9	3.7	0.28	2008.8	Olga-Noel 2007
12	14.99	1.74	5.46	112.1	519.9	129.7	38	132.8	630.5	6	1.49	2005.2	Alpha 2005
14	13.68	1.93	5.6	145.7	456.6	122.9	74.3	111.8	542.5	6.1	0.94	2004.5	Jeanne 2004
16	12.79	2.09	5.7	280.1	481.7	128.2	9.7	108.3	575.6	8	0.57	2003.5	
18	14.35	2	5.65	194.1	692.7	133.1	21.5	155.8	535.7	10.1	1.12	2001.7	
20	12.5	2.02	5.66	135.0	728.1	140.3	9.9	99.9	531.8	14.4	1	2000.8	
22	12.89	2.13	5.72	304.3	882.6	151.3	9.6	109.1	474.4	9	1.03	1999.9	George 1998
24	11.59	3.26	5.83	254.6	921.1	166.8	21.3	108.1	386.1	7.5	0.63	1998.9	
26	11.12	3.24	5.69	156.5	848.3	116.4	40.2	110.0	471	9.8	0.79	1997.3	Hortensia 1996
28	13	1.95	5.73	260.0	1041.7	131.2	9.5	127.5	472.4	10.9	0.57	1996.0	
30	12.12	2.15	5.67	214.3	901.7	108.1	9.4	121.6	386.4	3.7	0.52	1994.3	
32	13.33	2.26	6.06	265.3	1026.0	141.8	55.9	115.5	472.4	6.9	0.42	1992.3	
34	11.64	2.14	5.73	192.8	999.3	157	36.0	78.7	418.6	17	0.31	1990.0	
36	15.16	2.43	5.92	169.9	1132.1	137.3	38.3	131.3	316.8	11.1	0.38	1986.7	Emely 1987
38	11.27	2.25	5.91	258.6	1125.6	169.8	9.1	91.4	347.6	6.7	0.29	1984.1	
40	13.34	2.53	6.14	354.0	1006.6	155.1	21.0	61.8	419.8	5.9	0.29	1980.6	David Federico 1979
42	13.06	2.34	6	89.3	940.6	120.2	9.5	103.0	375.1	9.7	0.33	1977.2	
44	13.8	2.07	5.99	293.5	994.4	130.1	16.6	86.6	312.3	6.2	0.27	1974.2	
46	12.82	2.08	5.99	261.3	901.7	139.5	37.5	84.4	361.2	13.8	0.26	1970.5	
48	10.75	2.29	6.08	234.4	1079.0	163	55.9	105.4	250.9	9.7	0.17	1966.7	
60	13.52	2.31	6.13	278.8	1146.6	155.8	35.2	91.0	379	15.6	0.05	1960.9	
70	13.3	2.22	6.07	324.5	1244.2	95.6	9.6	93.4	331	10.3	0.02	1939.9	
80	13.51	2.36	5.91	309.7	1224.4	106.6	21.3	90.7	336	9	0.01	1898.9	

In the Samaná port (Samaná River), the C4 core was extracted, where calcium and iron decreased with depth (Table 6). Between 22–43 cm, a change in the sedimentation rate was observed (Figure 8). Of terrigenous influence, the Samaná River collects wastewater from Santa Bárbara de Samaná. Changes in the composition of the elements and the rate of sedimentary accumulation correspond to EWP (Figure 8).

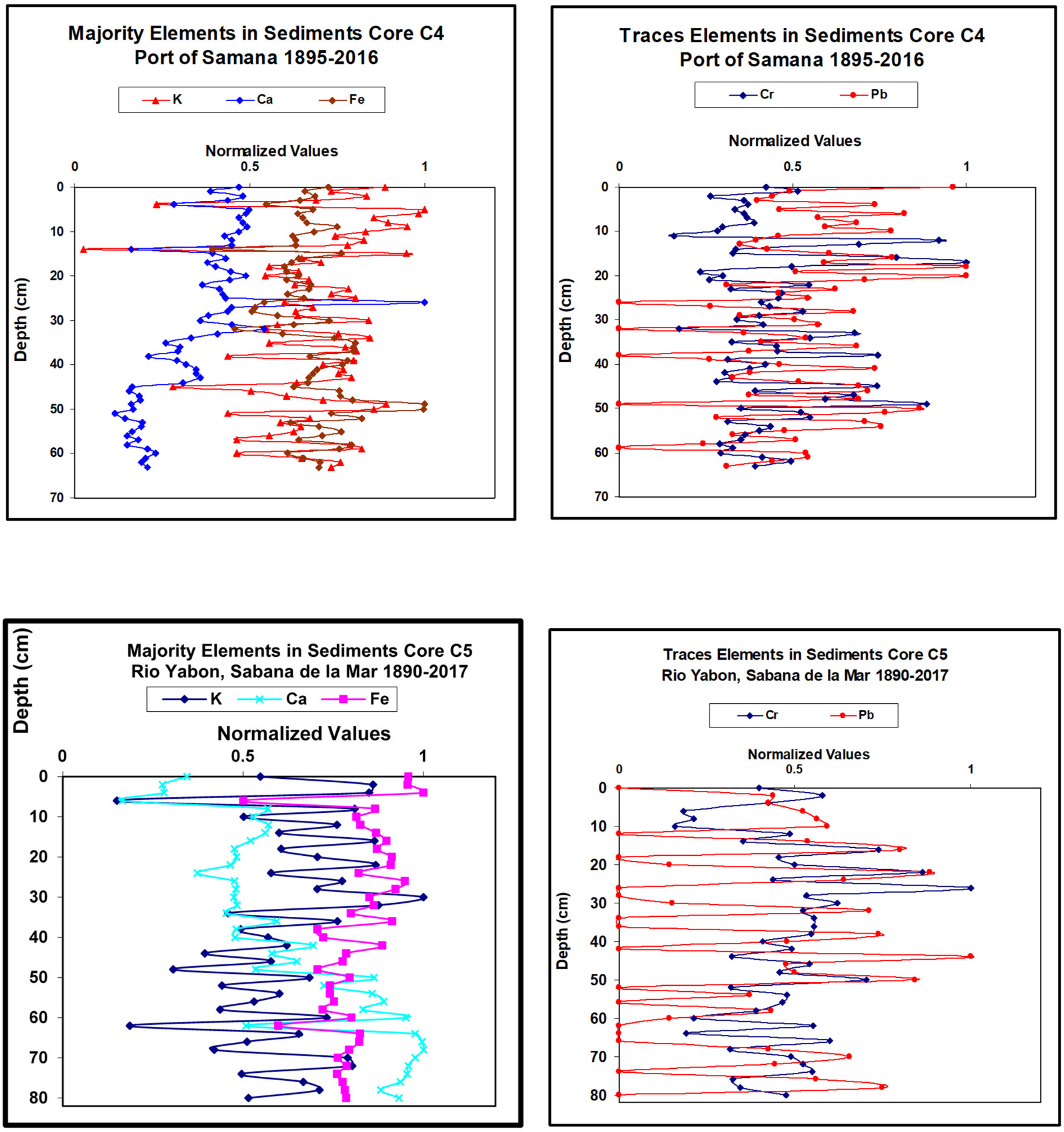

Figure 8. Relationship of the chemical elements with the depth in core C4 (majorities: potassium, calcium, and iron; minorities: chromium and lead). Core C5 (majority: potassium, calcium, and iron; minority: chromium and lead)

Table 5. Trace elements, Loss by ignition, % of Iron, % of Calcium, Sedimentation rate, Date, and EWP of the sections of the core C3 north of the city of Miches during the period from 1892–2016. We only consider the sections with higher values of lead at 3.9 µg/g

Proof. (cm)	**%PPI**	**%Ca**	**%Fe**	Cr µg/g	Mn µg/g	Ni µg/g	Cu µg/g	Zn µg/g	Br µg/g	Pb µg/g	TAS cm/a	Sedimentation date	Storm Date
0	11.97	42.89	0.65	10.9	159.5	28.7	18.4	36.8	166.9	7.6	1.90	2016.1	
2	10.81	41.75	0.59	5.5	133.4	36.9	8.8	37.5	142.3	6.3	0.51	2015.5	Bertha2014
4	13.55	43.00	0.68	27.3	148.3	31.3	6.7	33.2	122.2	4.7	0.35	2013.6	Gabrielle 2013
8	11.91	44.89	0.62	10.9	114.8	27.7	9.6	36.1	144.0	6.8	0.27	2009.8	Olga-Noel 2007
14	9.27	44.61	0.60	43.4	117.7	37.7	8.1	37.5	71.7	10.1	0.61	1999.8	
18	16.97	45.97	0.61	28.4	164.5	13.7	8.2	32.2	66.2	4.0	0.69	1995.4	Hortensia 1996
22	22.05	46.64	0.59	17.5	65.9	9.8	9.2	38.4	58.7	6.7	0.61	1992.3	
24	28.15	47.23	0.60	10.9	95.7	7.6	7.9	35.2	47.2	7.2	0.36	1990.6	Hugo 1989
26	9.33	35.67	0.60	30.5	52.2	39.6	8.0	32.9	64.2	9.2	0.44	1987.9	Emely 1987
32	13.93	49.16	0.60	18.5	61.3	46.4	7.4	33.6	65.8	5.6	0.20	1978.5	David Federico 1979
34	12.10	44.08	0.57	46.4	116.4	23.1	9.6	33.5	87.7	5.6	0.13	1973.5	
36	16.06	47.97	0.58	38.2	278.9	10.1	6.4	28.0	67.8	6.0	0.14	1965.8	
38	10.54	47.67	0.58	43.7	78.3	24.1	7.8	32.2	41.1	6.6	0.09	1958.6	
40	19.87	48.63	0.55	25.1	74.6	14.5	8.4	39.0	41.1	4.0	0.07	1947.4	
42	7.71	47.48	0.56	13.1	116.8	7.6	9.2	34.0	56.2	5.4	0.05	1932.4	
44	9.41	47.60	0.59	5.5	89.9	42.6	23.9	30.2	47.8	7.7	0.05	1911.7	
46	16.62	47.29	0.54	10.9	105.2	19.5	8.5	34.2	57.8	8.1	0.05	1892.5	

Table 6. Trace elements, Loss by ignition, % of Iron, % of Calcium, Sedimentation rate, Date, and EWP of the sections of the C4 core corresponding to the mouth of the Samaná River in the port of Samaná City during the period from 1895–2016. We only consider the sections with higher values of lead at 20 µg/g

Proof (cm)	%PPI	%Ca	%Fe	Cr µg/g	Mn µg/g	Ni µg/g	Zn µg/g	Br µg/g	Hg µg/g	Pb µg/g	TAS cm/s	Sedimentation date	Storm date
0	16.92	3.43	3.35	232.6	482.6	51.7	44.5	137.1		48.6	9.26	2016.5	
2	16.56	3.52	3.18	144.7	555.9	103.0	61.7	114.5		22.3	1.89	2016.0	
4	18.31	2.07	2.53	203.9	396.6	159.8	46.8	83.6		37.1	1.6	2015.3	Bertha 2014
6	16.75	3.58	2.95	197.9	428	114.1	40.8	89.8		41.5	7.12	2013.9	Gabrielle 2013
8	21.02	3.53	3.07	213.2	455	142.2	40.2	82.4		34.5	2.9	2013.6	
10	15.89	3.44	3.16	156.5	469	211.0	60.1	85.9		39.5	5.37	2013.0	Dorian 2012
14	16.62	1.2	1.82	184.3	142.1	110.5	27.9	64.4		21.5	3.46	2012.2	Maria 2011
15	13.93	2.88	3.52	180.6	505.7	66.0	65.4	74.8		30.5	3.35	2011.9	Irene 2011
16	13.87	3.16	2.96	439.4	432.3	183.6	37.9	69.1		39.7	2.85	2011.6	
18	15.36	2.94	2.78	274.1	414.7	233	41.7	62.3		50.4	2.99	2010.8	Earl 2010
21	13.4	3.25	2.8	142.4	443	133.7	37.4	59.4		35.7	3.43	2009.7	Henri 2009
24	12.92	3.1	2.81	257.9	376.2	189.9	39.5	59.8		23.1	1.83	2008.8	
28	9.9	3.21	2.34	291.7	406	193.8	29.8	48.3	4.2	34.1	1.4	2006.6	
30	12.4	2.64	3.36	186.9	492	156.6	34.5	57.1		25.5	1.14	2005.5	
31	12.03	3.29	2.89	228.1	447.9	174.1	35.7	46		28.9	1.48	2004.6	Jeanne 2004
34	13.4	2.44	3.43	302.4	499.1	120.8	56.3	49.3		27.2	0.81	2001.3	
36	13.51	2.21	3.68	248.9	507.4	87.8	54.1	48		34.5	0.56	1999.1	
40	13.19	2.34	3.54	232.2	454.1	160.6	50.4	46.8		23.3	0.72	1994.3	
41	13.2	2.54	3.2	207.9	541.7	100.5	56.3	51.6		37.1	1.42	1992.9	H. Klaus 1990
44	10.95	2.28	3.07	153.8	463.2	119.9	57.2	40.2		26.1	0.94	1987.1	Emily 1987
46	15.73	1.15	3.49	215.2	404.5	223.4	47.6	44.2	2.9	36.1	0.45	1984.1	
48	16.02	1.38	3.67	325.9	414.5	199.7	40.4	50.7		34.8	0.74	1980.9	David Federico 1979
50	14.09	1.23	4.61	193.2	285.2	154.4	53.6	43.4		43.7	0.36	1978.0	
51	14.93	0.86	3.38	287.8	228.6	145.4	28.3	42		38.6	0.58	1975.2	Eloise 1975
54	15.19	1.4	3.23	239.7	440	163.3	31.2	52.9		38.0	0.56	1965.8	Faith 1966
55	13.68	1.2	3.51	221.5	329.8	193.4	29	43.5		24.1	0.26	1964.0	
57	14.98	1.34	2.95	193.8	221	215.9	31.3	49		25.7	0.14	1955.9	
60	12.09	1.7	2.81	160.1	340.4	183.6	38.5	41.9		27.2	0.1	1937.2	
61	13.78	1.49	3.03	227.4	263.7	107.5	36.8	52.6		27.5	0.1	1927.3	
62	14.98	1.4	3.24	272.5	388.6	145.8	51.3	48.5		22.3	0.05	1917.6	

Table 7. Trace elements, Loss by ignition, % of Iron, % of Calcium, Sedimentation rate, Date, and EWP of the sections of the C5 core corresponding to the Yabón river mouth during the period from 1890–2017. We only consider the sections with higher values of lead at 10 µg/g

Proof (cm)	%PPI	%Ca	%Fe	Cr µg/g	Mn µg/g	Ni µg/g	Zn µg/g	Br µg/g	Pb µg/g	TAS cm/a	Sedimentation date	Storm date
2	16.44	1.03	4.94	158.7	725.1	93.5	22.4	86.0	11.8	1.27	2017.0	
4	14.56	1.05	5.16	116.4	716.7	32.3	28.1	82.1	11.5	0.92	2016.2	
6	19.98	0.62	2.59	49.9	346.7	51.8	8.3	88.9	14.1	2.90	2015.1	Bertha 2014
8	15.37	2.12	4.47	57.9	620.7	123.6	27.9	96.8	15.2	0.76	2014.8	Gabrielle 2013
10	20.78	1.96	4.20	44.0	678.9	74.5	11.8	97.5	16.0	0.58	2013.5	
14	17.92	2.09	4.49	96.9	660.8	17.3	24.5	87.2	14.5	2.08	2011.4	Irene 2011
16	16.85	1.94	4.63	202.3	679.4	87.5	34.2	92.2	21.6	1.30	2010.9	Earl 2010
22	18.26	1.74	4.70	236.9	530.9	62.4	27.8	81.3	23.9	2.46	2009.4	
24	20.24	1.39	4.24	119.8	547.4		29.0	76.9	17.3	1.55	2009.0	
32	17.10	1.80	4.45	143.7	637.1	87.8	22.4	73.4	19.2	1.18	2006.4	Rita 2005
38	19.89	1.79	3.64	150.3	578.9	72.4	12.6	76.4	19.9	0.98	2003.6	
40	18.40	1.78	3.73	112.3	489.7	35.4	11.8	72.2	12.9	1.07	2002.6	
44	18.33	2.16	4.06	87.8	620.0	60.4	21.4	89.3	27.0	1.14	2000.9	
46	19.06	2.42	4.00	148.2	545.9	65.0	27.9	80.1	12.8	1.23	2000.0	
48	19.23	2.00	3.65	125.1	530.6	93.0	25.6	79.9	13.5	0.65	1999.2	George 1998
50	18.73	3.22	4.11	192.7	581.8	75.2	24.2	82.0	22.7	0.64	1997.7	
54	22.99	3.20	3.83	131.1	625.9	53.7	21.6	85.0	10.0	0.76	1994.2	
58	18.54	3.11	3.72	107.2		119.0	25.4	77.8	11.7	0.68	1990.6	Klaus 1990
68	16.15	3.73	4.10	87.0	523.6		12.1	65.3	11.5	0.15	1972.1	
70	15.70	3.64	3.94	134.0	578.1	111.0	10.5	57.0	17.7	0.16	1965.3	
72	17.55	3.57	4.06	143.3	666.1	77.9	22.9	58.3	12.0	0.06	1959.0	
76	17.86	3.49	4.00	89.0	530.9		24.9	55.3	15.1	0.05	1932.0	
78	17.25	3.29	4.04	95.0	587.9	67.5	24.8	57.4	20.2	0.05	1911.0	

Table 8. Trace elements, Loss by ignition, % of Iron, % of Calcium, Sedimentation rate, Date, and EWP of the sections of the core C6 corresponding to the Caño Hondo river mouth, San Lorenzo Bay, during the period from 1922–2017. We only consider the sections with higher lead values at 5.0µg/g. In section 47 the increase in TAS could correspond to an older sediment mixture during earthquakes in the area in 1946

Proof (cm)	%PPI	%Ca	%Fe	Cr µg/g	Mn µg/g	Ni µg/g	Zn µg/g	Br µg/g	Pb µg/g	TAS cm/a	Sedimentation date	Storm daate
0	14.42	1.22	4.43	194	562.8	103.7	11.4	157.9	13.3	6.83	2016.9	
2	13.9	1.21	4.44	238.8	561.3	65.2	18	107.1	14.2	1.38	2016.2	
6	13.54	1.34	4.51	180.8	462.8	84.7	16.8	93.5	14.6	5.09	2013.3	Gabrielle 2013
10	13.38	1.26	4.62	247.8	453.8	57.1	10.7	90	16.5	3.79	2012.1	Dorian 2012
11	14.51	1.41	4.63	249.8	419.6	14.3	15.4	86.3	22.3	3.96	2011.8	Maria 2011
13	14.63	1.25	4.71	222.5	480.8	52.6	15.6	93.8	15.1	3.23	2011.2	Earl 2010
14	14.47	1.29	4.8	282.7	351.3	6.5	17.9	94.7	5.1	2.42	2010.9	
19	12.92	1.16	4.56	284.7	459.6	29.9	21.3	85.5	32.3	1.7	2008.4	Noel Olga 2007
20	13.79	1.3	4.64	158.7	445.8	17.9	9.6	86.6	18.1	1.88	2007.8	
31	10.84	1.29	4.64	351.3	543.6		4.6	66.5	20.9	0.91	1999.4	George 1998
32	10.74	1.14	4.65	250.8	491.4	26.2	15.6	59.3	16.8	0.44	1998.3	
34	11.09	1.21	4.88	228.7	510.2	4.4	12.3	58.5	29.9	0.46	1993.9	
35	10.37	1.23	4.66	208.1	536.7	27.2		57.8	11.8	0.57	1991.8	Klaus 1990
36	10.62	1.29	4.78	321.6	383.1	65.7	14.2	51.6	9.2	0.3	1990.0	
37	10.87	1.19	4.79	138.9	592.3	78.3	10	55.7	14.2	0.58	1986.7	
39	11.24	1.2	4.85	296.6	431.8		17.3	66.4	9.4	0.42	1982.9	Gert 1981
44	11.42	1.23	4.47	252.6	448.7	37.8	7.1	61.1	16.6	0.32	1963.1	H. Flora 1963
45	11.15	1.13	4.83	364.7	517.8	64.5	8.3	58.4	14.2	0.16	1959.9	
46	11.75	1.26	4.98	205.3	424.6	21.5	5.9	64.2	5.5	0.11	1953.6	
47	11.01	1.19	4.65	259.8	413.6	40.3	4.6	57.2	13.4	0.21	1944.9	Tsunami 1946

Table 9. Trace elements, Loss by ignition, % of Iron, % of Calcium, Sedimentation rate, Date, and EWP of the sections of the C7 core corresponding to the Yeguada river mouth in the city of Miches during the period from 1947–2017. We only consider the sections with higher values of lead at 5.0 µg/g

Proof (cm)	%PPI	%Ca	%Fe	Cr µg/g	Mn µg/g	Ni µg/g	Br µg/g	Hg µg/g	Pb µg/g	TAS cm/a	Sedimentation date	Storm date
0	11.08	16.36	1.34	75.9	411.8	101.1	23.6	2.7		1.46	2017.2	
1	11.51	18.47	0.89	52.2	325.3	125.7	19.6			0.52	2016.5	Bertha 2014
2	9.52	8.74	2.35	68.3	477.4	100.9	40.4		19.4	0.47	2014.6	
3	11.08	10.80	1.93	137.6	435.2	73.1	32.9	4.4	20.6	0.59	2012.4	
4	7.99	9.51	2.30	139.0	438.8	98.5	31.8		26.4	0.63	2010.8	
5	7.90	10.66	1.65	77.9	542.6	126.2	39.9		18.8	0.42	2009.2	
6	7.65	18.16	0.95	79.4	320.2	37.3	18.5		22.3	0.48	2006.8	Jeanne 2004
7	7.70	17.40	0.86	51.9	364.4	70.7	18.8			0.43	2004.7	
8	9.93	17.49	0.98	50.5	336.2	116.5	21.4		6.2	0.46	2002.4	Debby 2000
9	11.66	16.44	0.97	86.3	328.1	83.3	25.1			0.44	2000.2	
10	18.02	14.69	1.15	62.1	395.0	117.3	39.4		7.9	0.32	1997.9	George 1998
11	19.75	14.28	1.17	38.3	352.3	54.9	30.8			0.34	1994.7	
12	19.96	14.79	1.09	62.3	367.7	87.6	21.7			0.28	1991.8	Klaus 1990
13	22.62	14.03	1.05	60.0	353.4	119.0	28.5			0.18	1988.3	
14	24.43	15.36	1.02	50.8	395.5	74.0	25.9		13.7	0.18	1982.6	
15	19.56	14.71	1.06	21.4	417.3	77.7	29.6		11.7	0.12	1977.1	
16	20.34	15.01	0.91	106.2	424.4	76.1	21.9	5.0		0.11	1968.8	
17	18.24	15.11	1.05	35.7	385.6	89.5	21.9		14.1	0.08	1959.8	
18	14.39	15.79	1.20	47.4	459.1	71.6	28.1		14.6	0.05	1947.6	

The sedimentation between 0–33 cm is similar in relation to calcium and iron; from here until 45 cm, calcium increased, and iron decreased, changing more iron than calcium in the composition. Titanium, similar in nature to iron, diminishes toward the surface. Calcium and strontium, of a similar nature, follow the same trend, changing their relationship in the same sections as the other elements, according to the climatic conditions in the region of the port of Samaná. At 45–47 cm, there was a change in the sedimentation process. At this depth, the values of many elements tend to be constant.

The graphs that relate the TAS and EWP indicate that the Olga and Noel storms did not affect the north coast of the bay, unlike other EWP (Figure (8) due to the trajectory of these phenomena (NOAA, 2019). The most notable changes observed in the sedimentation regime of the C5 core are associated with Hurricane Debby, which occurred in the year 2000: calcium has replaced iron in recent years. Changes in composition also associated with EWP were observed at other depths (Scott et al., 2013). The Yabón River flows into this area, close to the municipality of Sabana de la Mar. After the Yuna, it deposits the most sediments in the bay (Figure 10). Its main basin, formed by karst and volcanic rocks, is in the eastern mountain range. The chemical elements of core C5 at 0–64 cm present changes; from 60 cm, the values remain constant, coinciding with the year 1990 and Hurricane Klaus. In the C6 core, the same process occurs with similar geological characteristics as in the C5 core. The sediments come from Los Haitises National Park, formed by karstic rocks, dragged by the Caño Hondo River, and deposited in San Lorenzo Bay. At the mouth of the La Yeguada River in Miches, the C7 core was taken, basically consisting of calcium carbonate. The majority elements vary according to the sedimentation rate, the EWP, and also the minorities of lead and chromium. Core C7 has the same behavior as cores C5 and C6. The changes in the sedimentation rate are related to meteorological eventualities.

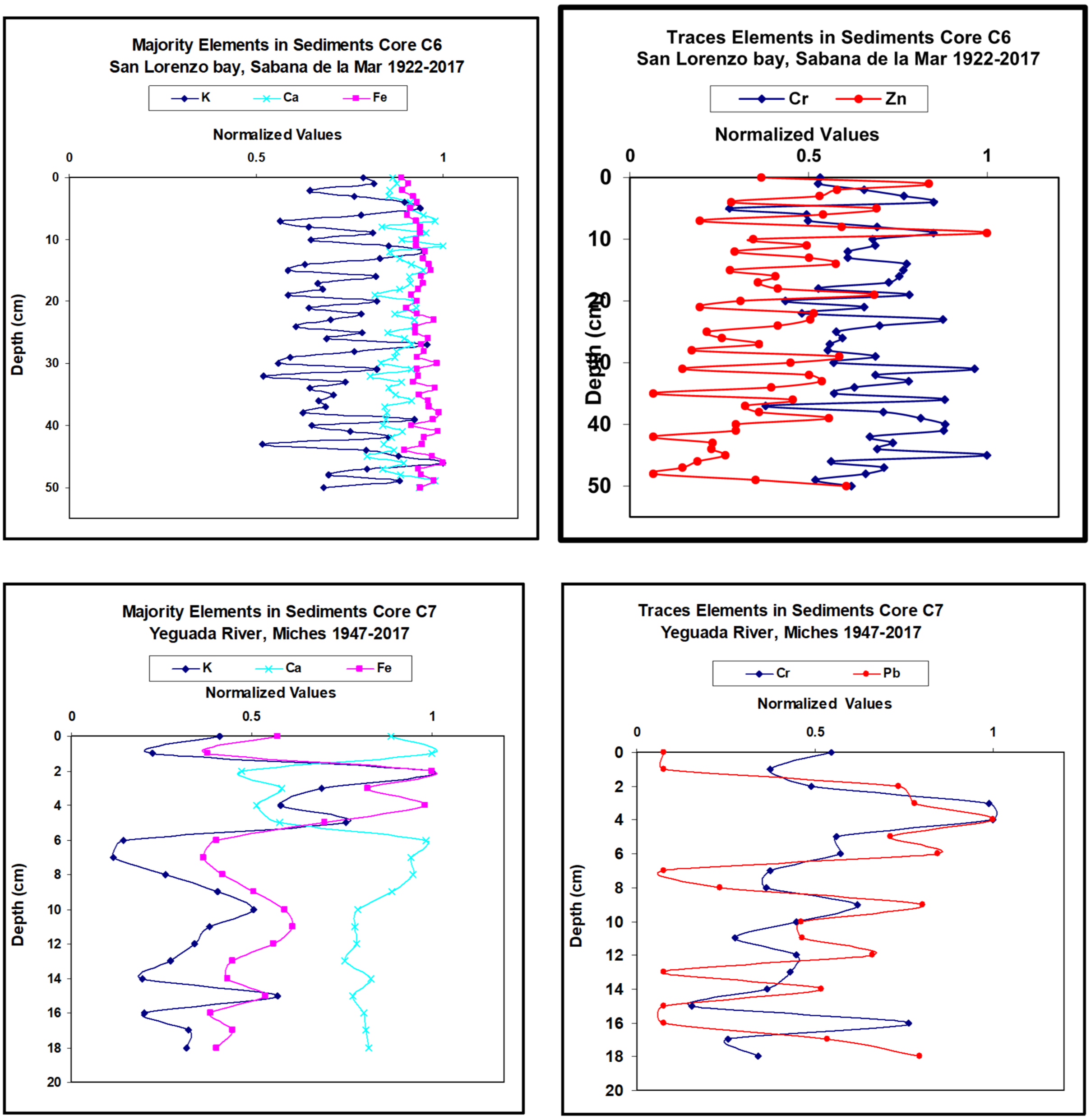

Figure 9. Relationship of the chemical elements with the depth in core C6 (majorities: potassium, calcium, and iron; minorities: chromium and lead). Core C7 (majority: potassium, calcium, and iron; minority: chromium and lead)

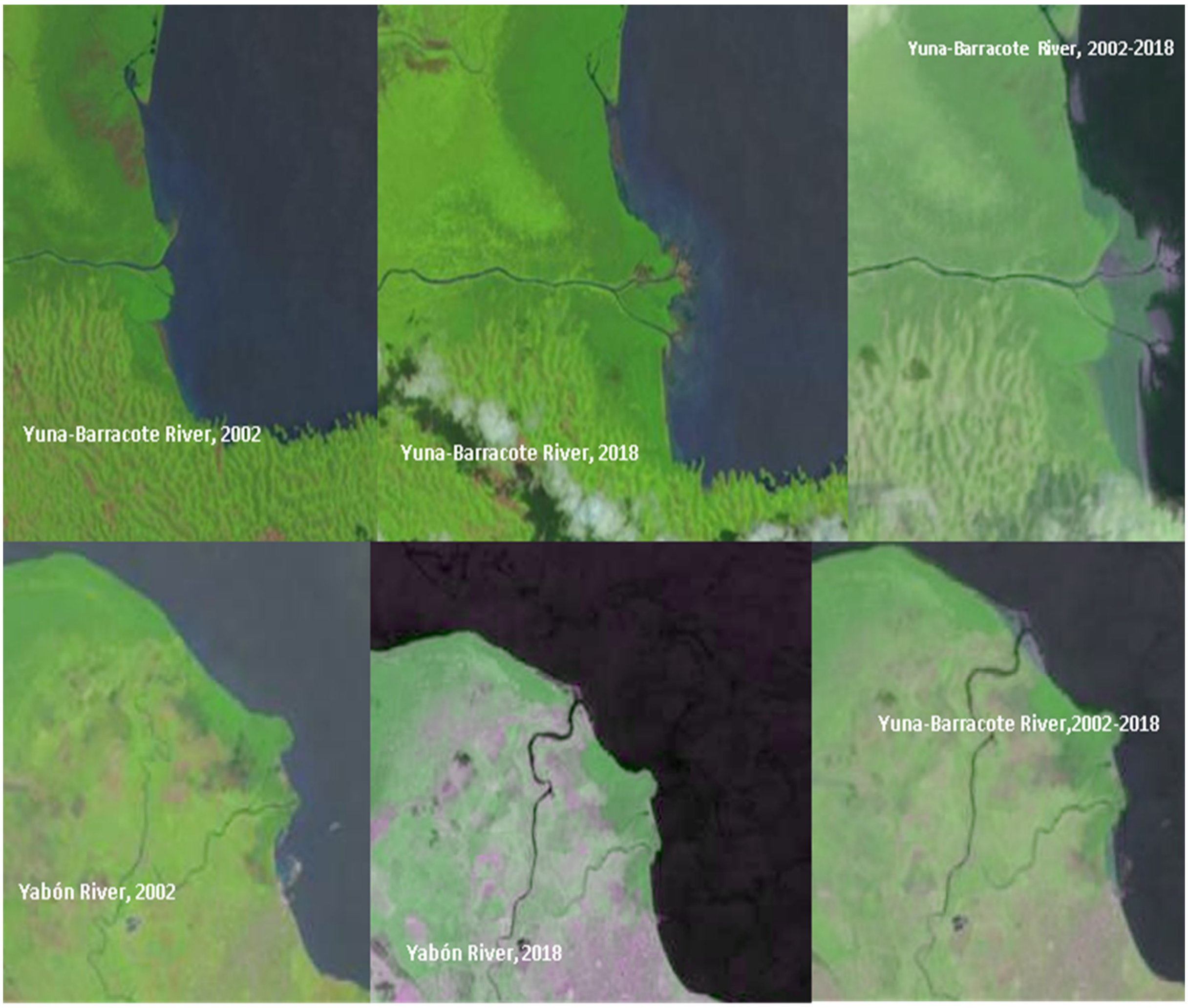

Figure 10. Morphology of the mouths of the Yuna-Barracote and Yabón rivers in 2002 and 2018. Variation of the coastline due to the high rate of sediment accumulation during the period 2002-2018. Source: Landsat 7 Satellite Images (2002) and Landsat 8 (2018)

4. Discussion

From the 90's, the EWPs have increased both in frequency and intensity (Goldenberg et al 2001, Villarini et al 2011) , because the TAS has also been increased in the Bay of Samaná. There are two other phenomena that have been developed in the DR that are the deforestation of Los Haitises National Park and the mining exploitation in Pueblo Viejo, Cotui.

The sediments, by their origin, contain heavy metals and an important amount of organic matter (from 15 to 24%). In the sediments contributed by the Yabón River, the content of organic matter has been decreasing, by which we can assume that this has been very quickly undermining its new channel when it is diverted. In the case of the Caño Hondo River, which flows into the bay of San Lorenzo, the content of organic matter varies between 10 and 15%. The sediments deposited by the rivers Yuna, Yabón, and La Yeguada have filled the lower parts (beaches) of the coastal area to the south of the bay which, added to the uprisings by the tectonic movements, have caused the land to enter the bay. The sediments deposited by the Yuna River during the period from 2003–2018 have occupied an area of 2.17 km^2 in the Bay of Samaná (Figure 9) while those deposited by the rivers Yabón and Yeguada occupy 0.08 km^2 and 0.06 km^2, respectively.

5. Conclusions

In the period from 2007–2016, a sediment deposit that reached 38 cm and a column of 12 cm was placed at about 4 km southeast of the municipality of Sánchez and east of the mouth of the Yuna River. In the bay of San Lorenzo, a column of 22 cm (2.2 km) from its mouth was deposited by the Caño Hondo River from Los Haitises.

In the port of Samaná, a column of more than 28 cm was deposited in the same period. At the mouths of all the rivers, streams, and gullies of the northern part of the bay, large amounts of sediment were also found. In this period, the storms Noel-Olga, (2007), Ike (2008), Henry (2009), Earl (2010), María-Irene (2011), Dorian (2012), Gabrielle (2013), and Bertha (2016) occurred. In 2017, hurricanes Irma and María hit the entire Samaná Bay, especially the La Yeguada river basin in Miches and deposited a quantity of sediment in the coastal zone.

The behavior of the sediments deposited in Samaná Bay by the rivers Yuna, Yabón, Caño Hondo, and La Yeguada are directly linked to EWP such as troughs and storms, as well as a decrease in these sediments, which can be observed when there are drought episodes (Figure 4). In the first depositions from EWP, the content of organic matter is higher than the next depositions by the trawls, this being recorded in the sediment rates and compositions. Abrupt changes in the rainfall regime produced an equal change in the estuary sedimentation regime, according to the 210Pb dating of Sánchez's core (Yuna-Barracote).

Acknowledgment

To the staff of the Ministry of Higher Education, Science and Technology. Autonomous University of Santo Domingo Dr. Plácido Gómez, MsC. Miledy Alberto, Ing. Alejandro Ozuna, Lic. Domingo Mercedes, Lic. Isabel Ulloa, Maestra Idalia Acevedo, Dr. Carlos Rodríguez, Dr. Carlos Alonso Hernández, MsC Zoraida Zapata, MsC. Miguel Batista, Lic. Marcos Casila, Msc. Nelphy de la Cruz, Yamileza Herrera, Queiroz Portorreal, Droniguiel Jiménez. José Osvaldo Suarez, Juan Pablo González.

References

Alonso Hernández, C. M., Díaz Asencio, M., Gómez Batista, M., Bolaños Alvares, Y., Muñoz Caravaca, A., & Morera Gómez, Y. (2016). Radiocronología de sedimentos marinos y su aplicación en la comprensión de los procesos de contaminación ambiental en ecosistemas marinos cubanos. *Nucleus*, (60), 35-40.

Bionini, W. E., Hargraves, R. B., & Shagan, R. (1984). The Caribean-South American Plata Boundary and Regional Tectonic. *Geological Society of America, Memoir*, *162*.

Bird, J. M. (1980). Plate tectonics: selected papers from publications of the American Geophysical Union. *Plate tectonics: selected papers from publications of the American Geophysical Union, by Bird, John M. Washington, DC: AGU, 1980.. American Geophysical Union.*

Brink, U. T., Danforth, W., Polloni, C., Andrews, B., Llanes, P., Smith, S., ... & Uozumi, T. (2004). New seafloor map of the Puerto Rico Trench helps assess earthquake and tsunami hazards. *Eos, Transactions American Geophysical Union*, *85*(37), 349-354. doi: 10.1029/2004EO370001. issn: 0096-3941.

Delanoy Ramón, A., & Méndez-Tejeda, R. (2017). Hydrodynamic Study of Lake Enriquillo in Dominican Republic. *Journal of Geoscience and Environment Protection, 5*, 115-124. doi: 10.4236/gep.2017.55009.

Delanoy, R. A. (1996). *Aspectos de sismología dominicana*. Ramon A Delanoy.

Díaz de Neira, J. A., & Hernaiz Huerta, P. P. (2004). Mapa Geológico de la Hoja a escala 1: 50.000 nº 6272-I (Antón Sánchez) y Memoria correspondiente. *Dirección General de Minería, Santo Domingo, 125p*.

Dolan, J. F., & Mann, P. (Eds.). (1998). *Active strike-slip and collisional tectonics of the northern caribbean plate boundary zone* (Vol. 326). Geological Society of America.

Eptisa. (2004). Programa SYSMIN. *Informe de la unidad hidrogeológica de la península de Samaná.*

Fernández-Domingo, J. I. (2010). Los Tesoros del Mar y su Régimen Jurídico. *Biblioteca Iberoamericana de Derecho.* Editorial Temis S.A. Bogotá, México D.F., Madrid, Buenos Aires, 2010.

Goldenberg, S. B., Landsea, C. W., Mestas-Nuñez, A. M., & Gray, W. M. (2001). The recent increase in Atlantic hurricane activity: Causes and implications. *Science*, *293*(5529), 474-479. doi: 10.1126/science.1060040

Hippensteel, S. P., Eastin, M. D., & Garcia, W. J. (2013). The geological legacy of Hurricane Irene: Implications for the fidelity of the paleo-storm record. *GSA Today*, *23*(12), 4-10.

IAEA. (1989). Isotopes of Noble gases as tracers in environmental studies. *Proceeding Consultants Meeeting, Vienna, 29 May-2 June 1989. Agency International.*

Lozano, R. L., San Miguel, E. G., & Bolívar, J. P. (2011). Assessment of the influence of in situ 210Bi in the calculation of in situ 210Po in air aerosols: Implications on residence time calculations using 210Po/210Pb activity ratios. *Journal of Geophysical Research: Atmospheres*, *116*(D8).

Mann, P., Burke, K., & Matumoto, T. (1984). Neotectonics of Hispaniola: Plate motion, sedimentation, and seismicity at a restraining bend. *Earth and Planetary Science Letters*, *70*(2), 311-324.

Mann, P., Shiroma, J., & Monechi, S. (1991). Sedimentologic, stratigraphic, and tectonic synthesis of Eocene-Miocene sedimentary basins, Hispaniola and Puerto Rico. *Geologic and tectonic development of the North America-Caribbean Plate boundary in Hispaniola*, *262*, 217.

NCA. (2018). Fourth National Climate Assessment. Retrieved from https://nca2018.globalchange.gov/chapter/20/

NOAA. (2019). Retrieved from https://www.nhc.noaa.gov/data/tcr/index.php?season=2007&basin=atl

Null, J. (2017). *El Niño and La Niña Years and Intensities. Based on Oceanic Niño Index (ONI), CCM.* Retrieved from https://ggweather.com/enso/oni.htm

Rodríguez Vegas, E., Gascó Leonarte, C., Schmid, T., Suárez, J. A., & Rodríguez Rastrero, M. (2014). Estudio preliminar sobre el uso de los radionucleidos ^{137}Cs y ^{210}Pb y las técnicas de espectrorradiometría como herramientas para determinar el estado de erosión de suelos. Retrieved from *http://www.iaea.org/inis/collection/NCLCollectionStore/_Public/45/012/45012641.pdf*

Salamanca, M., & Jara, B. (2003). Distribución y acumulación de plomo (Pb y 210Pb) en sedimentos de los fiordos de la XI Región. Chile. *Revista Ciencia y Tecnología del Mar*, *26*, 2.

Senz, J. G., Monthel, J., de Neira, J. A. D., Huerta, P. P. H., Viruete, J. E., & Estaun, A. P. (2007). La estructura de la Cordillera Oriental de la República Dominicana. *Boletín geológico y minero*, *118*(2), 293-311.

Villarini, G., Vecchi, G. A., Knutson, T. R., & Smith, J. A. (2011). Is the recorded increase in short-duration North Atlantic tropical storms spurious?. *Journal of Geophysical Research: Atmospheres*, *116*(D10).